Two-dimensional solitary pulses in driven diffractive-diffusive complex Ginzburg-Landau equations

Hidetsugu Sakaguchi

Department of Applied Science for Electronics and Materials, Interdisciplinary Graduate School of Engineering Sciences, Kyushu University, Kasuga 816-8580, Japan

Boris A. Malomed

Department of Interdisciplinary Studies, Faculty of Engineering, Tel Aviv University, Tel Aviv 69978, Israel

Abstract

Two models of driven optical cavities, based on two-dimensional Ginzburg-Landau equations, are introduced. The models include loss, the Kerr nonlinearity, diffraction in one transverse direction, and a combination of diffusion and dispersion in the other one (which is, actually, a temporal direction). Each model is driven either parametrically or directly by an external field. By means of direct simulations, stable completely localized pulses are found (in the directly driven model, they are built on top of a nonzero flat background). These solitary pulses correspond to spatio-temporal solitons ("light bullets") in the optical cavities. Basic results are presented in a compact form as stability regions in a full three-dimensional parameter space of either model. The stability region is bounded by two surfaces; beyond the left one, any two-dimensional (2D) pulse decays to zero, while quasi-1D pulses, representing spatial solitons in the optical cavity, are found beyond the right boundary. The spatial solitons are found to be stable both inside the stability region of the 2D pulses (hence, bistability takes place in this region in the two models) and beyond the right boundary of this region (although they are not stable everywhere). Unlike the spatial solitons, their quasi-1D counterparts in the form of purely temporal solitons are always subject to modulational instability, which splits them into an array of 2D pulses, that further coalesce into two final pulses. A uniform nonzero state in the parametrically driven model is also modulationally unstable, which leads to formation of many 2D pulses that subsequently merge into few ones.

1 Introduction

Complex Ginzburg-Landau (CGL) equations is a class of universal models describing pattern formation in media of various physical nature, combining nonlinearity with dissipative and dispersive linear properties. They find important applications to traveling-wave convection (see Ref. [1] and references therein), fiber optics [2], and in other fields. Nonlinear terms in a CGL equation, as well the linear ones, may be both dissipative, accounting for loss and gain, and conservative.

An important class of patterns that appear in different versions of the CGL equations are solitary pulses (SPs). In particular, a GL model with the cubicquintic (CQ) nonlinearity was first introduced by Petviashvili and Sergeev [3] in the two-dimensional (2D) case, with an objective to construct stable fully localized 2D pulses. The nonlinearity of the CQ type was necessary, as the stability of a pulse requires, first of all, the zero background to be stable, which implies that the linear part of the equation could not contain gain, hence a gain term had to be placed in the cubic nonlinearity. Finally, to provide for the overall stability of the model, the cubic gain had to be capped with a quintic lossy term.

Stable SPs ("solitons") in 2D CGL equations of various types were found in Refs. [4]. Stable axisymmetric solitons with an internal vorticity ("spin") have been found too in the isotropic CQ CGL equation [5]. On the other hand, the 2D CGL equation may find its most plausible experimental realization as a model governing evolution of optical spatiotemporal pulses in a planar nonlinear waveguide (2D optical cavity); in that case, however, the equation is strongly anisotropic due to the natural difference between the propagation direction (z)and the transverse one (x) along which the electromagnetic wave diffracts. In a rather general form, the corresponding anisotropic 2D model was put forward in Ref. [6]:

$$iu_{z} + \frac{1}{2}u_{xx} - (\frac{i}{2} + \beta)u_{tt} + \left[iu + (1 - i\gamma_{1})|u|^{2}u + i\gamma_{2}|u|^{4}u\right] = 0.$$
(1)

In this equation, u(z, x, t) is the local amplitude of the electromagnetic field, $t \equiv T - z/V_0$ is the so-called reduced time, where T is time proper, and V_0 is the group velocity of the carrier wave propagating in the z-direction [2]. Further, coefficients in front of the terms accounting for the transverse diffraction $(\frac{1}{2}u_{xx})$, linear loss (*iu*), optical filtering $(-\frac{1}{2}iu_{tt})$, which formally looks like diffusion in the t-direction), and Kerr nonlinearity $(|u|^2u)$ are all normalized to be 1. The remaining free parameters β , γ_1 , and γ_2 control the temporal dispersion, nonlinear cubic gain, and quintic loss (γ_1 and γ_2 must be positive, while β may have either sign or be equal to zero). SP solutions to Eq. (1) in the form $u(z, x, t) = \exp(ikz) v(x, t)$, with the function v(x, t) exponentially vanishing at $|x| \to \infty$ and $|t| \to \infty$, were found in Ref. [6], and their stability region was identified in the corresponding parameter space.

The model based on Eq. (1) assumes that the planar waveguide carrying the field is equipped with uniformly distributed linear *bandwidth-limited* gain (which induces the filtering term) combined with a saturable absorber [2], that together give rise to the CQ nonlinearity. For applications to nonlinear optics, it is also quite interesting to consider models where wave patterns are supported, instead of the intrinsic gain, by an external pump field, that leads to *driven* CGL equations, in which it is sufficient to take into regard the ordinary cubic (Kerr) nonlinearity, while the linear diffraction, dispersion, and filtering terms remain the same as in Eq. (1). In fact, two different driving terms may appear in the accordingly modified equation: a parametric drive and direct forcing, see below. It is quite interesting to find 2D spatiotemporal SPs in the driven optical models, as they have a real chance to be observed in the experiment, and are also of interest in their own right as completely localized pulses in the anisotropic 2D CGL equations of the new type.

In this work, we find these pulses and demonstrate their stability. Besides that, we also study quasi-1D solitons of two different types, which represent spatial and temporal solitons in the underlying optical models. It will be demonstrated that the spatial solitons are stable in a broad parametric region (although not everywhere); in particular, they coexist as stable attractors with the stable 2D pulses, hence both models are bistable in the corresponding regions. On the contrary to that, the temporal solitons are always modulationally unstable, and simulations show that the instability splits them into an array of 2D pulses, which subsequently coalesce into two 2D solitons. A uniform nonzero state in the parametrically driven model is also subject to modulational instability, which leads to a formation of a large number of 2D SPs; later, they merge into few final 2D solitons.

The rest of the paper is organized as follows. The two versions of the driven model are introduced in section 2, and SP solutions found in them are displayed in section 3. The results of extensive numerical simulations are summarized in the form of explicit stability diagrams in the corresponding three-dimensional parameter spaces. The paper is concluded by section 4.

2 The driven models

2.1 The parametric drive

In the 1D case, the parametrically driven CGL equation takes the form which generalizes the earlier studied parametrically driven damped nonlinear Schrödinger (NLS) equation (see Ref. [7], in which exact SP solutions to the latter equation were found, and their stability was investigated, and further results in Refs. [8]). The generalization to the 2D case of the same type as in Eq. (1), which describes a planar waveguide (optical cavity) with the Kerr nonlinearity, is straightforward:

$$iu_z + \frac{1}{2}u_{xx} - (\frac{i}{2} + \beta)u_{tt} + \frac{1}{2}|u|^2 u = (k - i)u + \gamma u^*,$$
(2)

where the asterisk stands for the complex conjugation. The gain, which is accounted for by the last term in Eq. (2) with a real coefficient γ is provided by a pump wave copropagating with the *u*-field at the double frequency. The real coefficient *k* determines a wavenumber mismatch between the signal and pump waves. Dropping the filtering term and assuming $\beta < 0$ (which physically corresponds to anomalous dispersion of the electromagnetic waves in the waveguide [2]) transform Eq. (2) into a 2D isotropic damped parametrically driven NLS equation, which is used as a phenomenological model of the Faraday ripples in hydrodynamics [9], in which case the evolutional variable z in Eq. (2) is replaced by time T, and the former temporal variable t is replaced by the second transverse coordinate y. A more general isotropic equation, which includes the diffusion term,

$$iu_{z} + (\frac{1}{2} - iD)\nabla^{2}u + \frac{1}{2}|u|^{2}u = (k - i)u + \gamma u^{*}, D > 0,$$
(3)

is also used as a model to describe localized 2D states, the so-called oscillons, observed in experiments with the Faraday resonance [10]. Getting back to the damped isotropic NLS equation with the parametric drive, we note that this equation (with the evolutional variable z) finds applications to the description of spatial patterns in 3D driven optical cavities [11]. In a recent preprint [12], it has been shown that axisymmetric solitons may be stable in the latter model, despite the presence of the collapse in its undamped undriven version (which is the NLS equation proper).

In the present work, the objective is to find stable SPs in the strongly anisotropic full CGL model (2), which will have the meaning of *spatiotemporal* optical solitons [13] propagating in the planar waveguide. It seems obvious that pulses may only exist if the gain parameter exceeds the loss coefficient, i.e., $\gamma > 1$. On the other hand, an obvious necessary condition for the stability of pulses is the stability of the zero background against perturbations of the form

$$u = a \exp\left(\sigma z + iqx - i\omega t\right) + b \exp\left(\sigma^* z - iqx + i\omega t\right) \tag{4}$$

with infinitesimal amplitudes a and b, where q and ω are arbitrary real wavenumber and frequency of the perturbation. A dispersion relation which determines the (complex) instability growth rate σ as a function of q and ω can be easily found from the linearized equation (2):

$$\left(\frac{1}{2}q^2 - \beta\omega^2 + k\right)^2 + \left[\left(\operatorname{Re}\sigma + 1 + \frac{1}{2}\omega^2\right) + i\operatorname{Im}\sigma\right]^2 = \gamma^2,\tag{5}$$

which gives rise to two different branches of the dispersion relation, viz., $\operatorname{Re} \sigma = -\left(1 + \frac{1}{2}\omega^2\right)$ with $\operatorname{Im} \sigma \neq 0$, and the one with $\operatorname{Im} \sigma = 0$ and σ determined by the equation

$$\left(\sigma + 1 + \frac{1}{2}\omega^2\right)^2 = \gamma^2 - \left(\frac{1}{2}q^2 - \beta\omega^2 + k\right)^2.$$
 (6)

Obviously, the former branch always satisfies the stability condition, $\operatorname{Re} \sigma(q, \omega) \leq 0$. Straightforward analysis of Eq. (6), with regard to the above assumption

 $\gamma > 1$, shows that, if $\omega = 0$, the stability condition for the latter branch amounts to the well-known inequalities [7, 8] $\gamma^2 \leq 1 + k^2$, k > 0.

The consideration of Eq. (6) with $\omega \neq 0$ demonstrates that, in this case, the most dangerous perturbations are those with q = 0. If $\beta \leq 0$, they do not generate any additional instability, and if β is positive, a new stability condition appears, $\gamma^2 \leq (k+2\beta)^2/(1+4\beta^2)$; it is easy to check that the above-mentioned necessary condition $\gamma^2 \leq 1 + k^2$ is a straightforward corollary of this inequality. Thus, the eventual system of the conditions providing for the stability of the zero solution to Eq. (2) (provided that the system is infinitely extended in both x- and t-directions) is $k \geq 0$ and

$$\gamma^{2} \leq 1 + k^{2}, \quad \text{if } \beta \leq 0; \\ \gamma^{2} \leq (k + 2\beta)^{2} / (1 + 4\beta^{2}), \quad \text{if } \beta > 0.$$
 (7)

It is also relevant to consider nonzero spatially uniform solutions to Eq. (2), which have the form

$$u = A_0 \exp(i\phi), \ \phi = -\frac{1}{2}\sin^{-1}(1/\gamma), \ A_0 = \sqrt{2\left[k + \gamma\cos(2\phi)\right]}.$$
 (8)

This uniform solution exists for $\gamma > 1$. The consideration of the modulational stability of the solution against small perturbations with the wavenumber q and instability growth rate σ (cf. Eq. (4)) yields a dispersion relation

$$\left(\frac{1}{2}q^2 - \beta\omega^2 + k - A_0^2\right)^2 + \left[\left(\operatorname{Re}\sigma + 1 + \frac{1}{2}\omega^2\right) + i\operatorname{Im}\sigma\right]^2 = \gamma^2 - \gamma A_0^2 \cos(2\phi) + A_0^4/4$$

As well as Eq. (5), this equation has a solution branch with $\text{Im } \sigma = 0$, then

$$\sigma = -1 - \omega^2 / 2 \pm \sqrt{\gamma^2 - \gamma A_0^2 \cos(2\phi) + A_0^4 / 4 - (q^2 / 2 - \beta \omega^2 + k - A_0^2)^2}.$$
 (9)

The maximum value of this expression, which is attained at $\omega = 0$ and $q = \sqrt{2(k - A_0^2)}$, is always positive, $\sigma_{\text{max}} = -1 + \sqrt{1 + k^2}$. Therefore, the uniform state (8) is always unstable against modulations in the *x*-direction, the same way as in the 1D damped parametrically driven NLS equation [7, 8].

2.2 The directly forced model

The light signal in a lossy waveguide can also be directly (rather than parametrically) supported by a pump wave launched at the same (rather than double) frequency. For spatial patterns in 3D lossy optical cavities (a typical example is a domain wall [14]), this gives rise to the well-known isotropic directly forced 2D CGL equation, with the propagation coordinate z playing the role of the evolutional variable, see a review [15] (a similar model describes a cavity with a trapped Bose-Einstein condensate in the presence of source and sink of atoms [16]). The optical patterns generated this way may find an application in the design of optical memory [17], although fully localized pulses may be subject to collapse under the action of the self-focusing Kerr nonlinearity [18].

The governing equation for the spatiotemporal optical signal in the directly forced nonlinear waveguide differs from Eq. (2) by the driving term:

$$iu_z + \frac{1}{2}u_{xx} - (\frac{i}{2} + \beta)u_{tt} + \frac{1}{2}|u|^2 u = (k - i)u - f,$$
(10)

where f is the amplitude of the forcing field. Obviously, this equation can only produce localized patterns on top of a constant background $u \equiv u_0$, whose amplitude is determined by a cubic equation following from Eq. (10), $(1/2) |u_0|^2 u_0 + (i - k) u_0 + f = 0$. The background can be subject to modulational instability [2]; however, if the amplitude u_0 is small enough, the instability will be so weak that it may be disregarded for finite values of the propagation distance that are relevant to the experiment.

3 Numerical results

3.1 Two-dimensional pulses in the parametrically driven model

Equations (2) and (10) were solved numerically by means of a pseudospectral code with 256×256 modes and periodic boundary conditions in x and t, with a fixed size of the system in both directions, $L_x = L_t = 20$. As well as in Ref. [6], a stable 2D SP was generated for the first time, starting with an initial Gaussian pulse localized in both x and t, with its center placed at the center of the integration domain. In order to generate stability diagrams (see below), we then varied the parameters by small steps, the initial configuration for each simulation being the stable pulse produced by the simulation at the previous step.

In Fig. 1 we display a typical example of a stable 2D completely localized pulse, which was produced by the numerical solution of Eq. (2), following the procedure outlined above. Results of extensive simulations, which were carried out for many different values of the parameters, can be presented in a compact form as a stability diagram for the 2D pulses in the three-dimensional parametric space (γ, k, β) , which is displayed in Fig. 2. We stress that this parameter space comprises all the coefficients of Eq. (2).

The stability region proper is located under the "roof" in Fig. 2. To the left of the stability border which is shown by crosses, no localized 2D pulses can be created: in this case, an initial 2D pulse configuration quickly decays into the stable zero state. On the other side, i.e., to the right of the border denoted by rhombuses, localized 2D pulses were not found either. However, the result of the evolution is different in this case: the initial 2D pulse expands along the

t-axis to generate a quasi-1D pulse, which is localized in the x-direction, and delocalized in the t-direction. Such a quasi-1D solution to Eq. (2) can be found in an exact form,

$$u(x,t) = \sqrt{2\kappa}e^{i\phi}\operatorname{sech}(\kappa x), \ \phi = -\frac{1}{2}\sin^{-1}(1/\gamma), \ \kappa = \sqrt{2\left[k + \gamma\cos(2\phi)\right]}.$$
(11)

In terms of the underlying optical models, the solution (11) corresponds to a *spatial* soliton. A typical example of such a soliton is shown in Fig. 3. Straightforward comparison shows that the numerically found quasi-1D pulse completely coincides with the analytical solution (11). Simulations demonstrate that this spatial soliton is stable everywhere in the stability region of the 2D pulses shown in Fig. 2, i.e., the model is *bistable* in this region. Beyond the right stability border of the 2D pulses, shown by rhombuses in Fig. 2, i.e., in the region where only the spatial solitons are found, they remain stable.

For comparison with these results, we have also performed direct simulations of the isotropic equation (3). Stable 2D localized pulses exist in this model too, Fig. 4 displaying an example for D = 0.1. For D = 0.1 and k = 1.3, the stable axially symmetric 2D pulses have been found in the interval $1.20 < \gamma < 1.57$. For $\gamma < 1.20$, the initial 2D pulse decays to the zero state, while for $\gamma > 1.57$ the initial 2D pulse evolves to the spatially uniform state (8). In this connection, we note that a critical branch of the modulational-instability growth rate for this uniform solution to Eq. (3) can be found, as a function of the perturbation wavenumber q, in the form $\sigma(q) = -1 - Dq^2 + \sqrt{1 + k^2 - (q^2/2 + k - A_0)^2}$, cf. Eq. (9). It is easy to check that, for D = 0.1 and k = 1.3, $\sigma(q)$ is negative for any q, hence the uniform state is stable.

3.2 Modulational instability of quasi-one-dimensional pulses in the parametrically driven model

In the context of the results presented above, the spatial solitons (quasi-1D pulses) were stable. However, they become unstable against t –dependent perturbations for sufficiently large negative values of the dispersion coefficient β in Eq. (2), which corresponds to anomalous dispersion in terms of nonlinear optics (in fact, modulational instability of spatial solitons against temporal perturbations in a system with anomalous dispersion is a general effect which has been known for a long time [19]). In particular, for k = 1.3 and $\gamma = 1.3$, this instability occurs if $\beta < -1.08$. Figure 5 displays a result of numerical simulations in this case. The initial condition including a small perturbation is taken as

$$u(x,t,z=0) = \sqrt{2\kappa} \left[\left(1 + 0.05 \cos\left(\frac{8\pi t}{L}\right) + 0.01 \cos\left(\frac{2\pi t}{L}\right) \right) \cos\phi + i \sin\phi \right] \operatorname{sech} \left(\kappa \left(x - \frac{L}{2} \right) \right) \right] \operatorname{sech} \left(\kappa \left(x - \frac{L}{2} \right) \right) + \left(12 \right) \operatorname{sech} \left(\kappa \left(x - \frac{L}{2} \right) \right) \right] \operatorname{sech} \left(\kappa \left(x - \frac{L}{2} \right) \right) + \left(12 \right) \operatorname{sech} \left(\kappa \left(x - \frac{L}{2} \right) \right) \right) = \left(12 \right) \operatorname{sech} \left(\kappa \left(x - \frac{L}{2} \right) \right) + \left(12 \right) \operatorname{sech} \left(\kappa \left(x - \frac{L}{2} \right) \right) \right) = \left(12 \right) \operatorname{sech} \left(\kappa \left(x - \frac{L}{2} \right) \right) + \left(12 \right) \operatorname{sech} \left(\kappa \left(x - \frac{L}{2} \right) \right) \right) = \left(12 \right) \operatorname{sech} \left(\kappa \left(x - \frac{L}{2} \right) \right) = \left(12 \right) \operatorname{sech} \left(\kappa \left(x - \frac{L}{2} \right) \right) = \left(12 \right) \operatorname{sech} \left(\kappa \left(x - \frac{L}{2} \right) \right) = \left(12 \right) \operatorname{sech} \left(\kappa \left(x - \frac{L}{2} \right) \right) = \left(12 \right) \operatorname{sech} \left(\kappa \left(x - \frac{L}{2} \right) \right) = \left(12 \right) \operatorname{sech} \left(\kappa \left(x - \frac{L}{2} \right) \right) = \left(12 \right) \operatorname{sech} \left(\kappa \left(x - \frac{L}{2} \right) \right) = \left(12 \right) \operatorname{sech} \left(\kappa \left(x - \frac{L}{2} \right) \right) = \left(12 \right) \operatorname{sech} \left(\kappa \left(x - \frac{L}{2} \right) \right) = \left(12 \right) \operatorname{sech} \left(\kappa \left(x - \frac{L}{2} \right) \right) = \left(12 \right) \operatorname{sech} \left(\kappa \left(x - \frac{L}{2} \right) \right) = \left(12 \right) \operatorname{sech} \left(\kappa \left(x - \frac{L}{2} \right) \right) = \left(12 \right) \operatorname{sech} \left(\kappa \left(x - \frac{L}{2} \right) \right) = \left(12 \right) \operatorname{sech} \left(\kappa \left(x - \frac{L}{2} \right) \right) = \left(12 \right) \operatorname{sech} \left(\kappa \left(x - \frac{L}{2} \right) \right) = \left(12 \right) \operatorname{sech} \left(\kappa \left(x - \frac{L}{2} \right) \right) = \left(12 \right) \operatorname{sech} \left(\kappa \left(x - \frac{L}{2} \right) \right) = \left(12 \right) \operatorname{sech} \left(\kappa \left(x - \frac{L}{2} \right) \right) = \left(12 \right) \operatorname{sech} \left(\kappa \left(x - \frac{L}{2} \right) \right) = \left(12 \right) \operatorname{sech} \left(\kappa \left(x - \frac{L}{2} \right) \right) = \left(12 \right) \operatorname{sech} \left(\kappa \left(x - \frac{L}{2} \right) \right) = \left(12 \right) \operatorname{sech} \left(\kappa \left(x - \frac{L}{2} \right) \right) = \left(12 \right) \operatorname{sech} \left(\kappa \left(x - \frac{L}{2} \right) \right) = \left(12 \right) \operatorname{sech} \left(\kappa \left(x - \frac{L}{2} \right) \right) = \left(12 \right) \operatorname{sech} \left(\kappa \left(x - \frac{L}{2} \right) \right) = \left(12 \right) \operatorname{sech} \left(\pi \left(x - \frac{L}{2} \right) \right) = \left(12 \right) \operatorname{sech} \left(\pi \left(x - \frac{L}{2} \right) \right) = \left(12 \right) \operatorname{sech} \left(\pi \left(x - \frac{L}{2} \right) \right) = \left(12 \right) \operatorname{sech} \left(\pi \left(x - \frac{L}{2} \right) \right) = \left(12 \right) \operatorname{sech} \left(\pi \left(x - \frac{L}{2} \right) \right) = \left(12 \right) \operatorname{sech} \left(\pi \left(x - \frac{L}{2} \right) \right) = \left(12 \right) \operatorname{sech} \left(\pi \left(x - \frac{L}{2} \right) \right) = \left(12 \right) \operatorname{sech} \left(\pi \left(x - \frac{L}{2} \right) \right) = \left(12 \right) \operatorname{sech} \left(\pi \left(x - \frac{L}{2} \right) \right) = \left(12 \right) \operatorname{sech} \left(\pi \left(x - \frac{L}{2}$$

where κ and ϕ are the same constants as in Eq. (11). Figure 5(a) displays the evolution of |u(x = L/2, t)| at $\beta = -2.5$. While the pattern remains localized in

the *x*-direction during the evolution, it is obvious in Fig. 5(b) that the growth of the modulation splits the original spatial soliton into four 2D spatiotemporal pulses, but three of them merge together, thus two 2D pulses survive (splitting of a spatial solitary beam into temporally localized pulses under the action of modulational instability was earlier observed in numerical [20, 21] and laboratory [21] experiments with second-harmonic-generating optical systems). Figure 5(b) displays an eventual established state including the two 2D pulses. This modulational instability is a generic type of transverse instability for quasi-1D pulses (another generic type is the zigzag instability found in Ref. [6] in the context of the 2D GL equation with the CQ nonlinearity).

Another type of quasi-1D pulse solution to Eq. (2), which is localized in the *t*-direction and uniform in the *x*-direction, is also possible. Such an *x*independent solution, u(z, t, z) = U(z, t), represents a *temporal* soliton in the optical cavity, and satisfies the equation

$$iU_z - (\frac{i}{2} + \beta)U_{tt} + \frac{1}{2}|U|^2 U = (k - i)U + \gamma U^*$$
(13)

(an exact analytical solution to this equation is not available, unless $\beta = 0$). For the same case, k = 1.3 and $\gamma = 1.3$, as considered above, this type of the quasi-1D pulse solution exists and is stable against *t*-dependent perturbations if $\beta < -0.812$. Figure 6(a) displays such a pulse at $\beta = -1, k = 1.3$ and $\gamma = 1.3$, with its center at the point t = L/2. To study its stability against *x*-dependent perturbations, we took an initial condition

$$u(x, t, z = 0) = [1 + 0.05 \cos(2\pi x/L)] \operatorname{Re} U(t) + i \operatorname{Im} U(t),$$

where U(t) is the unperturbed z-independent SP solution to Eq. (13). Modulation in the x- direction grows and splits the temporal soliton into many 2D spatiotemporal pulses, as it is evident in Fig. 6(b), which displays a 3D plot of |u(x,t,z)| at z = 200. Such a temporal soliton, extended along the x-direction, seems to be always unstable against the x-dependent perturbations, breaking up into a large number of 2D pulses.

One can also look for more general quasi-1D pulses of the form u(x, t, z) = U(x-ct), which may be interpreted as either moving spatial solitons, or oblique temporal ones, the function U satisfying an equation

$$(1 - 2c^2\beta - ic^2)U'' + |U|^2U = 2(k - i)U + 2\gamma U^*.$$

A detailed study of such general quasi-1D solitons is beyond the scope of this work, but one may assume that there is a critical value of the velocity c separating completely unstable solutions and those which may be stable.

We have also simulated the development of the modulational instability of the spatially uniform state (8) in the parametrically driven model (2) (the presence of this instability was demonstrated analytically in the previous section). Formation of many 2D pulses may be expected, at sufficiently small β , as a result of the instability development. As an initial condition, we took the uniform state (8) randomly perturbed by an initial small disturbance. Figure 7 displays a snapshot of the pattern obtained at z = 600 for $\beta = -2.5$, k = 1.3and $\gamma = 1.3$. At first, many 2D pulses are created; however, they subsequently merge, so that only a few 2D pulses eventually survive, which is obvious in Fig. 7.

3.3 The directly forced model

Numerical simulations of the directly driven CGL equation (10) also readily produce stable 2D pulses (built on top of the small-amplitude background, see above). A typical example of such a pulse is shown in Fig. 8. As well as in the parametrically driven model, in this case extensive simulations of Eq. (10) have made it possible to identify a stability region for 2D SPs in the full three-dimensional parameter space of the model, (f, k, β) . This region is located under the "roof" in the parameter space, see Fig. 9. Note that the parameter space in Fig. 9, as well as that in Fig. 2, incorporates all the parameters of the model.

The two boundaries of the stability region in Fig. 9 have the meaning similar to that of the stability boundaries shown in Fig. 2 for the parametrically driven model: to the left of the boundary shown by crosses, any initial pulse decays to zero, and to the right of the second boundary, shown by rhombuses, the fully localized 2D pulse evolves to a quasi-1D pulse oriented along the t-axis (the spatial soliton, in terms of the underlying optical models). As well as in the parametrically driven model, in the directly forced one the spatial solitons coexist as stable patterns with the 2D pulses (hence, the model is bistable in that region), and they remain stable across the right border of the stability region of the 2D solitons, i.e., across the surface shown by rhombuses in Fig. 9.

4 Conclusion

In this work, we have introduced two different two-dimensional models of the Ginzburg-Landau type with the Kerr (cubic) nonlinearity. The corresponding equations are driven either parametrically or directly by an external field. The models describe spatio-temporal dynamics in nonlinear dispersive lossy optical cavities, where the loss also includes a filtering term. Both models are strongly anisotropic, featuring only diffraction in one (spatial) direction, and a combination of effective diffusion and dispersion in the other (temporal) direction. By means of direct simulations, we have found stable two-dimensional solitary pulses in both models (in the directly driven one, the pulses are built on top of a nonzero flat background). These two-dimensional solitary pulses correspond to spatio-temporal solitons ("light bullets") supported by the driving field in the planar nonlinear waveguide.

The main results were presented in a compact form as stability regions in the full three-dimensional parameter space of either model. The stability region is bounded by two surfaces. Beyond one of them, any initial pulse decays to zero, while stable quasi-one-dimensional pulses, extending along the temporal direction (i.e., spatial solitons, in terms of the optical cavity), were found beyond the other boundary. The spatial solitons are also stable inside the stability regions of the two-dimensional pulses, so that both models demonstrate bistability in these regions. Unlike the spatial solitons, their quasi-one-dimensional counterparts in the form of temporal solitons are always modulationally unstable. It was demonstrated that the instability splits temporal solitons into an array of spatiotemporal two-dimensional pulses, which, in turn, coalesce into two final pulses. Similarly, the instability of the uniform nonzero state in the parametrically driven model leads to formation of many two-dimensional pulses, which subsequently merge into few two-dimensional solitons.

References

- H. U. Voss, P. Kolodner, M. Abel, and J. Kurths, Phys. Rev. Lett. 83, 3422 (1999).
- [2] G. P. Agrawal. Nonlinear Fiber Optics (Academic Press: San Diego, 1995)
- [3] A. M. Sergeev and V. I. Petviashvili, Dokl. AN SSSR 276, 1380 (1984)
 [Sov. Phys. Doklady 29, 493 (1984)].
- [4] O. Thual and S. Fauve, J. Phys. (Paris) 49, 1829 (1988); R. J. Deissler and H. R. Brand, Phys. Rev. A 44, R3411 (1991).
- [5] L.-C. Crasovan, B. A. Malomed, and D. Mihalache, Phys. Rev. E 63, 016605 (2001).
- [6] H. Sakaguchi and B. A. Malomed, Physica D 159, 91 (2001).
- [7] I. V. Barashenkov, M. M. Bogdan, and V. I. Korobov, Europhys. Lett. 15, 113 (1991).
- [8] I. V. Barashenkov and Yu. S. Smirnov, Phys. Rev. E 54, 5707 (1996); N. V. Alexeeva, I. V. Barashenkov, and D. E. Pelinovsky, Nonlinearity 12, 1 (1999).
- [9] D. Astruc and S. Fauve, Fluid Mechanics and Its Applications 62, 39 (2001).
- [10] P. B. Umbanhowar, F. Melo and H. L. Swinney, Nature 382, 793 (1996).

- [11] V. J. Sanchez-Morcillo, I. Perez-Arjona, F. Silva, G. J. de Valcarel, and E. Roldan, Opt. Lett. 25, 957 (2000); D. Gomila, P. Colet, G. L. Oppo, and M. San Miguel, Phys. Rev. Lett. 87, 4101 (2001).
- [12] I. V. Barashenkov, N. V. Alexeeva, and E. V. Zemlyanaya, "Two and three-dimensional oscillons in nonlinear Faraday resonance", e-print nlin.PS/0112047 (2001).
- [13] X. Liu, L.J. Qian, and F.W. Wise, Phys. Rev. Lett. 82, 4631 (1999); X. Liu, K. Beckwitt, and F.W. Wise, Phys. Rev. E 61, R4722 (2000).
- [14] S. Residori, P. L. Ramazza, E. Pampaloni, S. Boccaletti, and F. T. Arecchi, Phys. Rev. Lett. **76**, 1063 (1996); M. Hoyulos, P. Colet, M. San Miguel, and D. Walgraef, Phys. Rev. E **58**, 2992 (1998); G. Izus, M. San Miguel, and M. Santagiustina, Opt. Lett. **25**, 1454 (2000).
- [15] F. T. Arecchi, A. Boccaletti, and P. L. Ramazza, Phys. Rep. **318**, 1 (1999).
- [16] F. T. Arecchi, J. Bragard, and L. M. Castellano, Opt. Commun. 179, 149 (2000).
- [17] W. J. Firth and A. J. Scroggie, Phys. Rev. Lett. 76, 1623 (1996).
- [18] W. J. Firth and A. Lord, J. Mod. Opt. 43, 1071 (1996).
- [19] A.A. Kanashov and A.M. Rubenchik, Physica D 4, 122 (1981).
- [20] S. Trillo and M. Haelterman, Opt. Lett. **21**, 1114 (1996).
- [21] X. Liu X, K. Beckwitt K, and F. Wise, Phys. Rev. Lett. 85, 1871 (2000).

Figure Captions

Fig. 1. An example of the stable stationary two-dimensional solitary pulse, found as a solution of the parametrically driven complex Ginzburg-Landau equation (2). The field |u| is shown vs. the temporal and transverse spatial coordinates t and x. Values of the parameters are $k = 1.3, \beta = -0.3, \gamma = 1.30$.

Fig. 2. The region of stable two-dimensional solitary pulses in the full parameter space of Eq. (2). The stability region is located under the "roof". To the left of stability region, only zero solution is possible, and to the right of it, the 2D pulse evolves to a stable quasi-one-dimensional pattern, see an example in Fig. 3.

Fig. 3. An example of a stable quasi-one-dimensional pulse found in the parametrically driven complex Ginzburg-Landau equation (2). Values of the parameters are $k = 1.3, \beta = -0.3, \gamma = 1.36$ (a point corresponding to these values is located slightly to the right of the stability region shown in Fig. 2).

Fig. 4 An example of a stable axisymmetric two-dimensional solitary pulse found as a solution of the parametrically driven isotropic complex Ginzburg-Landau equation (3). The field |u| is shown vs. the temporal and transverse spatial coordinates. Values of the parameters are k = 1.3, D = 0.1 and $\gamma = 1.30$.

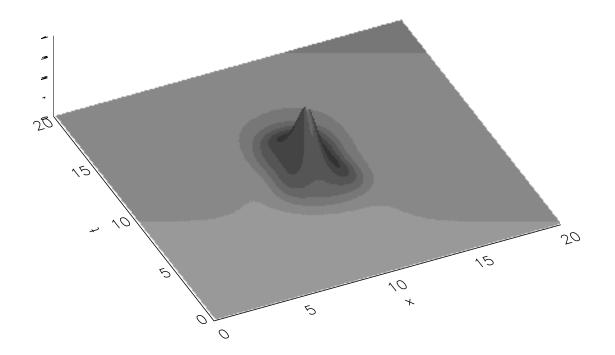
Fig. 5 (a) Evolution of |u(L/2, t, z)| for the parametrically driven complex Ginzburg-Landau equation (2). The initial state is a 1D localized pattern (12) (spatial soliton) including a small modulational perturbation, values of the parameters being $k = 1.3, \beta = -2.5, \gamma = 1.3$. (b) The established stationary pattern including two 2D pulses.

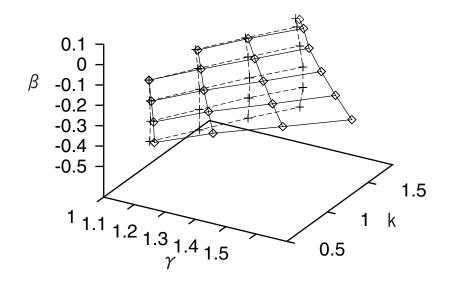
Fig. 6 (a) The quasi-one-dimensional pulse, which is localized in the t-direction around t = L/2 (temporal soliton), at $\beta = -1, k = 1.3$ and $\gamma = 1.3$, in the parametrically driven complex Ginzburg-Landau equation (2). (b) The result of the instability development of this soliton, shown as a plot of |u(x,t)| at z = 200.

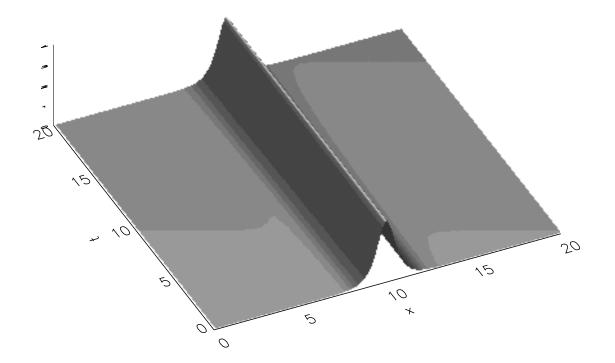
Fig. 7 Patterns produced by the modulational instability of the uniform state in the parametrically driven complex Ginzburg-Landau equation (2) at z = 600. Values of parameter are $\beta = -2.5$, k = 1.3 and $\gamma = 1.3$.

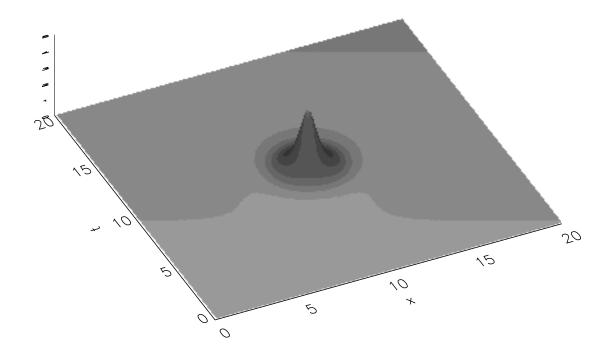
Fig. 8. An example of the stable stationary two-dimensional solitary pulse, found on top of the nonzero flat background, in the directly forced complex Ginzburg-Landau equation (10). The field |u| is shown vs. the temporal and transverse spatial coordinates t and x. Values of the parameters are $k = 3, \beta = -0.3, f = 3.1$.

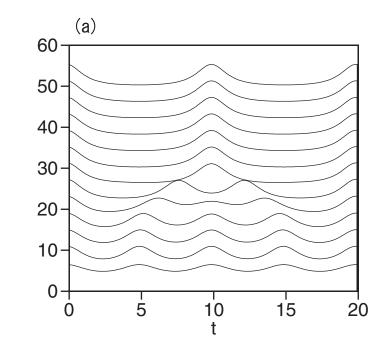
Fig. 9. The region of stable two-dimensional solitary pulses (built on top of the nonzero flat background) in the full parameter space of the directly forced complex Ginzburg-Landau equation (10). The stability region is located under the "roof". To the left of stability region, the 2D pulse decays to the flat-background solution, and to the right of the stability region, the 2D pulse evolves to a stable quasi-one-dimensional pattern (spatial soliton).











Ν

